

The effect of the aerodynamic behaviour of flakes of jarrah and karri bark on their potential as firebrands

P F M Ellis

CSIRO Sustainable Ecosystems
Climate Adaptation Flagship
PO Box 284, Canberra, ACT 2601, Australia
✉ peter.ellis@csiro.au

Manuscript received July 2009; accepted January 2010

Abstract

Spotting, the process by which new fires are ignited ahead of bushfires by firebrands transported by convection and wind, is a significant problem for fire suppression, and potentially, for fire crew safety. The magnitude of the potential problems caused by spotting is determined by many factors, notably spotting distance and spotfire numbers. This paper explains the notoriety of two Western Australian forest eucalypts, jarrah (*E. marginata*) and karri (*E. diversicolor*), in terms of bark aerodynamic characteristics and likely firebrand yield.

Terminal velocity, the equilibrium falling velocity, and potentially, gliding behaviour, determine how high a particle is likely to be lofted for given convection strength, and how far it will travel for a given height and wind conditions. Particles with low terminal velocities can potentially be lofted to greater heights and transported longer distances than those with greater terminal velocities. The gliding and spin behaviour of shed flakes of bark were observed during tower drops, and their terminal velocities derived from fall time.

Terminal velocity varied between 2.5 and 8 m s⁻¹ and is shown to be a function of the square root of surface density (mass/projected area) of the sample, the amount of spin during free-fall, and bark shape. Bark flakes which showed rapid spin had terminal velocities up to 18% less than those of non-spinning flakes. The measurements indicate that many of these flakes could be lofted in the convection plumes of low to medium-intensity fires, such as those with fire-front intensities between 0.5 and 2.5 MW m⁻¹. Aerodynamic characteristics which would make these bark flakes effective firebrands appear to be their low terminal velocities, rather than their ability to glide.

Observed differences in spotting behaviour between the two species are their spotting densities and maximum spotting distances. These differences are not wholly explained by their measured differences in free-fall behaviour, but will more completely be explained by differences in the numbers of detachable flakes, their ease of ignition and their combustion characteristics during flight.

Keywords: bushfire; firebrands; terminal velocity; spotting; coefficient of drag; surface density.

Introduction

The phenomenon of spotting, where pieces of burning material, firebrands, are lofted by the convection of a bushfire to start new fires down wind (McArthur 1967, Tolhurst and MacAulay 2003), is the main characteristic of forest fires that determines whether or not the fire can be suppressed (McCarthy and Tolhurst 1998). Potentially, spotting can lead to entrapment and expose fire crews to grave danger. The worst cases of spotting behaviour in the world both in terms of distance and spotfire concentration occur in Australia, and this has been attributed to the aerodynamic and combustion characteristics of eucalyptus bark (McArthur 1967, Cheney & Bary 1969, Luke & McArthur 1978).

Terminal velocity and shape are important characteristics of potential firebrand material that determine if it will be lofted in a bushfire plume (Tarifa *et al.* 1965, 1967, Lee and Hellman 1969). Particle terminal

velocity is its equilibrium falling speed in still air, and in order to be lofted by a fire, must be less than plume updraft velocity. The updraft velocities modelled for plumes from line fires with intensities of 0.5 MW m⁻¹ and 2.5 MW m⁻¹ are 4.0 m s⁻¹ and 6.9 m s⁻¹, respectively (Raupach 1990). These intensities correspond to a low-intensity fire at the upper limit recommended for prescribed burning, and a medium-intensity fire at the threshold at which direct suppression by bulldozers and aerial attack may fail.

There is considerable literature on the terminal velocities of prepared and natural wood samples (Tarifa *et al.* 1965; 1967, Muraszew 1974, Muraszew *et al.* 1975; 1976, Muraszew & Fedele 1976, Albin 1979) but little on bark (Muraszew *et al.* 1976, Clements 1977, Ellis 2000).

Terminal velocity can be obtained in five ways:

- derived from a standard drag relationship; or
- derived from measurements of drag vectors of tethered particles for a range of constant horizontal air velocities (Muraszew 1974, Muraszew *et al.* 1975, Tarifa *et al.* 1965, 1967); or

- directly measured for untethered particles in a vertical wind tunnel (Ellis 2000); or
- estimated from images which show fall relative to reference points (Clements 1977); or
- calculated from drop time (Clements 1977).

During free-fall objects tend to orient themselves so that their maximum projected area (A) is normal to the relative airflow (Tarifa *et al.* 1967), and at their terminal velocity, mass forces equal drag forces. Terminal velocity (w) is proportional to, the square root of surface density (m/A) and designated ' α ' here, and inversely proportional to the square root of coefficient of drag ($C_d^{0.5}$). Determining terminal velocity using a drag relationship requires the measurement of particle mass, projected area and the value for coefficient of drag. The last is dependent on shape, velocity, surface roughness and ambient turbulence and, for standard shapes, can be obtained from engineering tables (Marks 1951). However, firebrands are typically irregular in shape, with rough surfaces, and their projected area will vary if they gyrate during flight. Hence, deriving accurate values for terminal velocity using a standard drag relationship can be problematic. The second method requires very accurate measurement and the assumption that the particle will have a constant orientation during flight. In a vertical wind tunnel, many untethered particles such as bark flakes have a horizontal vector of velocity, due to glide, which results in impact with the walls. The fourth method is also difficult with particles which glide. The drop method allows observations for a limited time of particles which are free to gyrate naturally, and a simple calculation of terminal velocity, and was adopted for this study.

The aim of this study was to compare the terminal velocities, flight behaviour and likely firebrand yield of bark of two species of eucalypt with different bark physical characteristics and spotting behaviour, karri and jarrah.

The shed bark of karri (*Eucalyptus diversicolor* F. Muell.), a gum bark type, is a supposed agent of long-distance spotting to several kilometres (McCaw 1992, White¹ *pers. comm.* 1996). Karri has gum bark which decorticates seasonally in thin irregular flakes which can be more than 1000 mm long. Mature karri forest produces about 1.5 t ha⁻¹ of bark fall (O'Connell and Menagé 1982), and at any given time an unknown proportion of this would be loosely attached to the trunk or branches, and thus represent potential firebrands.

Jarrah, (*Eucalyptus marginata* Don ex Smith) has a fibrous bark type, is notorious for intense short-distance spotting to tens of metres, and less frequent spotting to one or two kilometres (McArthur 1967, Gould *et al.* 2008). Jarrah does not decorticate seasonally and large quantities of loosely attached flat or curved flakes of fibrous bark, typically up to 300 mm long, but occasionally more than 1000 mm long and 100 mm wide, accumulate on long-unburnt boles and branches. Medium-intensity fires of about 3 MW m⁻¹ burning in mature northern jarrah forest consume between 6 and 8 t ha⁻¹ of bark from the trunks, (Gould *et al.* 2008), and an unknown proportion of this would become firebrands.

Methods

Bark samples

Shed samples found at the base of about six karri and jarrah trees were collected respectively from the Manjimup and Nannup areas in Western Australia. Typically, karri flakes were curled tangentially and were irregular cylindrical or curved pieces. Typically, the jarrah flakes were more uniform in shape than those of karri, and were approximately rectangular and flat, or slightly curved longitudinally. Twenty-two karri and 27 jarrah samples were considered a sufficient number to capture variation.

Samples were weighed fresh and their length to width ratio ($L:W$) calculated. Each flake was placed on a sheet of paper in its estimated flight orientation and the projected area traced, cut out and weighed. Scanning was not used because of the curvature of the bark. Area A was calculated from the known mass per unit area for the sheet of paper. The root of surface density (m/A) was then calculated.

Drop tests

Bark samples were oriented such that their flat or convex surface faced the ground and dropped from a 22.7 m mobile tower in calm conditions and their fall time recorded using a stopwatch. The flight behaviour for each sample was subjectively categorized according to how rapidly they rotated while falling. Samples that rotated rapidly about an imaginary axis perpendicular to their flat surface or rapidly about their longitudinal axis were categorized 'Spin'. Those samples that showed no spin or rotated slowly were classed as 'No-spin'. 'Spin' and 'No-spin' were ascribed the values 1 and zero, respectively. The occurrence of spiral movement was noted and the diameter of the spiral estimated visually. The terminal velocity (w , m s⁻¹), termed observed terminal velocity, was calculated using Equation 1 (Clements 1977);

$$w = \frac{gt - \sqrt{g^2 t^2 - 4gy \ln 2}}{2 \ln 2} \quad \text{Eqn 1}$$

where g is acceleration due to gravity (9.8 m s⁻²), t is the fall time (s) and y is the height (m) from which the sample is dropped. The dimensionless coefficient of drag (C_d) for each sample was then derived using a standard approximation of a drag relationship for falling objects (Equation 2),

$$w = \left(\frac{2gm}{C_d A \rho_a} \right)^{0.5} \quad \text{Eqn 2}$$

where w is terminal velocity obtained from Equation 1, m is mass (kg), A is the maximum projected area (m²) which is the area normal to the airflow, and ρ_a is the density of air (1.27 kg m⁻³ at the site).

Data analysis

Initially, the data was plotted to show the significance of root of surface density (α) as a determinant of terminal velocity. Subsequently, correlation and anova were used to determine if there were additional explanatory

¹ Kevin White, formerly Regional Fire Coordinator, Central Forest Region, Dept. of Conservation Land Management, W.A.

Table 1

Length, length to width ratio ($L:W$), mass, projected area and square root of surface density of the bark samples. Mean (in bold), standard deviation, and range.

Species	Length (cm)	$L:W$	Mass (g)	Projected area (cm ²)	Root of surface density (kg ^{0.5} m ⁻¹)
Karri (n=22)	36.18 ± 11.75 (17.5–63.0)	11.71 ± 6.27 (5.1–26.5)	14.70 ± 9.77 (4.3–40.3)	98.38 ± 58.90 (18.7–213.11)	1.25 ± 0.28 (0.79–1.85)
Jarrah (n=27)	27.22 ± 9.38 (12.0–46.0)	11.27 ± 5.86 (2.0–30.0)	8.88 ± 10.93 (0.85–42.00)	77.81 ± 67.47 (14.13–267.10)	0.96 ± 0.29 (0.53–1.79)

variables for observed behaviour. Linear regression was used to obtain models for terminal velocity.

Results

Bark morphology

Bark morphology is described in Table 1.

Sample gyration

All samples appeared to assume an attitude of maximum drag, where the maximum surface area was presented to the relative wind (ie facing the ground), whatever their initial orientation. Most samples established a stable flat spin which could be fast or slow. Nearly all samples described a spiral glide but no samples glided in one direction for the duration of their flight. During the 22.7 m drop, the maximum amplitude of spiral flight in the horizontal plane, observed from above, was estimated to be less than 10 m.

Explanatory variables

The correlation matrix for measured bark variables and observed free-fall behaviour is shown in Table 2.

Correlations between mass and area, length and area and length and width occur because these variables tend to be linked via sample size. The coefficients also indicate that karri and jarrah samples differ in mass, α , length, and in observed spin. Terminal velocity appears to depend on mass, α and spin, and differs between species. Spin differs between species and is weakly associated with mass and $L:W$, and more strongly associated with terminal velocity and the coefficient of drag. Similarly, the coefficient of drag is associated with amount of spin observed, terminal velocity and $L:W$.

Significance of root of surface density

Figure 1 plots terminal velocity (w) versus the square root of surface density (α), indicating species and 'Spin', and Equation 3, which was obtained using constrained linear regression.

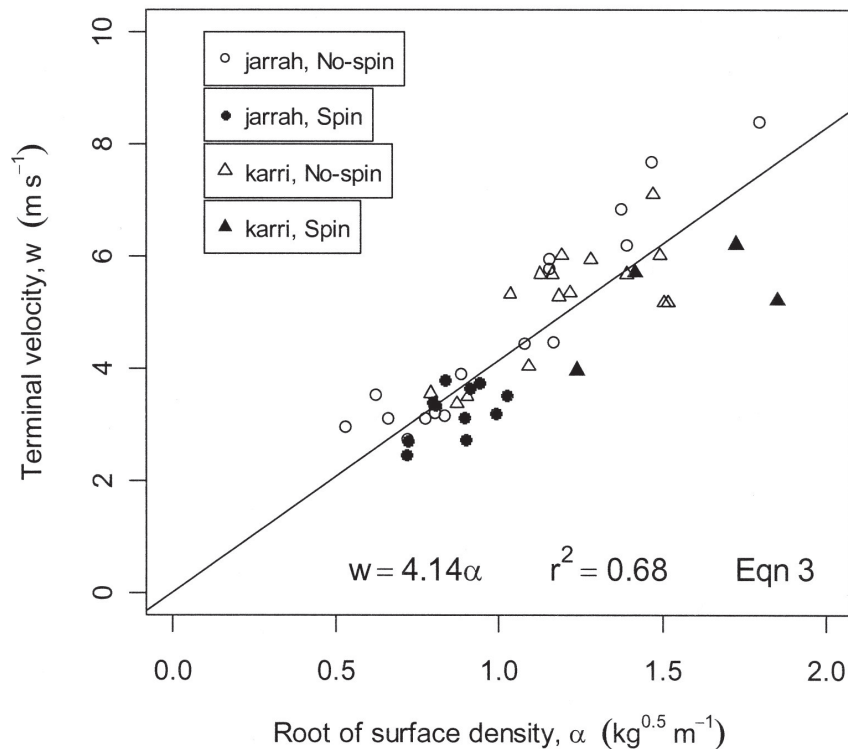


Figure 1. Relationship between the terminal velocity of shed flakes of karri and jarrah bark and the square root of surface density of each piece, indicating samples which displayed Spin during flight. Equation 3 describes the relationship between terminal velocity and the root of surface density.

Table 2

Correlation coefficients for the measured bark variables, observed spin behaviour, observed terminal velocity calculated using Equation 1, and the coefficient of drag derived using Equation 2. Values in bold are referred to in the text.

	Species	<i>m</i>	<i>A</i>	α	<i>L</i>	<i>W</i>	<i>L:W</i>	<i>w</i>	<i>Spin</i>
Mass (<i>m</i>)	-0.27	1.00							
Area (<i>A</i>)	-0.16	0.76	1.00						
Root surface density (α)	-0.45	0.59	0.10	1.00					
Length (<i>L</i>)	-0.40	0.56	0.59	0.33	1.00				
Width (<i>W</i>)	-0.12	0.75	0.85	0.16	0.34	1.00			
<i>L:W</i>	-0.04	-0.31	-0.42	0.09	0.27	-0.60	1.00		
Terminal velocity, obs. (<i>w</i>)	-0.35	0.60	0.15	0.84	0.21	0.17	-0.05	1.00	
<i>Spin</i> , ascribed 1 or 0	0.24	-0.23	-0.16	-0.08	-0.02	-0.19	0.28	-0.36	1.00
Coefficient of drag (<i>Cd</i>)	-0.05	-0.05	-0.03	0.16	0.15	0.01	0.21	-0.37	0.57

The spread of values in Figure 1 indicates that the karri and jarrah samples have different ranges in root of surface density and terminal velocity, and that samples with Spin tend to have lower terminal velocities than predicted by Equation 3. However, α is shown to be a significant explanatory variable of terminal velocity.

Differences between species

More than 35% of jarrah samples exhibited Spin, and all of these had relatively low values for α . Less than 20% of karri samples exhibited Spin, and all of these were in the upper half of the range of values for α . The means and ranges of area, α , terminal velocity and derived coefficient of drag for the No-spin and Spin categories illustrate differences between species (Table 3). Differences between means were tested using a standard ‘t’ test.

It was considered that there were sufficient differences between species to analyse them separately. For jarrah, linear regression resulted in Equation 4;

$$w(\text{jarrah}) = 4.62 \alpha - 0.74 \text{ Spin} \quad \text{Eqn 4}$$

$r^2 = 0.89$ (s.e. = 0.38) (s.e. = 0.22)
($P < 0.00001$) ($P = 0.004$)

where *w* is terminal velocity (m s^{-1}), α is root of surface

density ($\text{kg}^{0.5} \text{m}^{-1}$) and Spin and No-spin are ascribed the values of one and zero, respectively.

For karri, linear regression resulted in an expression which included α ($p=0.0004$), mass ($p=0.025$), Spin ($p=0.037$), and all four interactions ($p\sim 0.04$), and with a value for R^2 of 0.66. It is likely that because the karri samples varied in shape, and hence coefficient of drag, they showed more variability in response to surface density than did the jarrah samples. In order to remain consistent and avoid complexity, and at the cost of some precision, Equation 5 was obtained.

$$w(\text{karri}) = 4.29 \alpha - 1.40 \text{ Spin} \quad \text{Eqn 5}$$

$r^2 = 0.51$ (s.e. = 0.67) (s.e. = 0.48)
($P < 0.001$) ($P = 0.04$)

For Equations 3 to 5, the intercept was not found to be significant. The coefficients in Equations 4 and 5 are not significantly different. Figure 2 plots observed terminal velocities vs terminal velocities predicted using Equations 4 and 5 for jarrah and karri samples, respectively.

Terminal velocity was adequately predicted by variables measured surface density and observed Spin (Equations 4 and 5, Figure 2).

Table 3

The mean (bold), standard deviation and range for length to width ratio (*L:W*), length (*L*), projected area (*A*), root of surface density (α), terminal velocity (*w*) and derived coefficient of drag (*Cd*) for the species and spin data subsets. Significant differences (standard ‘t’ test, $P < 0.05$) between means of species is indicated ‘a’, and between categories of spin but within species, is indicated ‘b’.

No-spin						
	<i>L:W</i>	<i>L</i> (cm)	<i>A</i> (cm ²)	α ($\text{kg}^{0.5} \text{m}^{-1}$)	<i>w</i> (m s^{-1})	<i>Cd</i>
Karri	10.53 ± 5.72 (5.1–26.5)	36.00 ± 1.55 (17.5–63.0) a	109.17 ± 59.54 (18.7–213.1) b	1.18 ± 0.24 (0.79–1.52) b	5.11 ± 1.08 (3.36–7.10)	0.85 ± 0.23 (0.58–1.33) b
Jarrah	10.20 ± 4.79 (2.0–19.0)	26.28 ± 9.76 (12.0–42.0) a	76.72 ± 63.02 (14.1–216.8)	1.03 ± 0.36 (0.53–1.79)	4.72 ± 1.84 (2.73–8.39) b	0.77 ± 0.21 (0.48–1.07) b
Spin						
Karri	17.00 ± 6.68 (9.0–23.0)	37.00 ± 14.45 (27.0–58.0)	49.82 ± 18.90 (29.7–73.8) b	1.56 ± 0.28 (1.24–1.85) a, b	5.27 ± 0.96 a (3.97–6.22)	1.39 ± 0.43 b (0.95–1.95)
Jarrah	12.84 ± 7.09 (5.0–30.0)	28.6 ± 9.09 (17.0–46.0)	79.40 ± 76.64 (19.6–267.1)	0.86 ± 0.10 a (0.72–1.02)	3.25 ± 0.45 a, b (2.46–3.80)	1.13 ± 0.29 b (0.74–1.66)

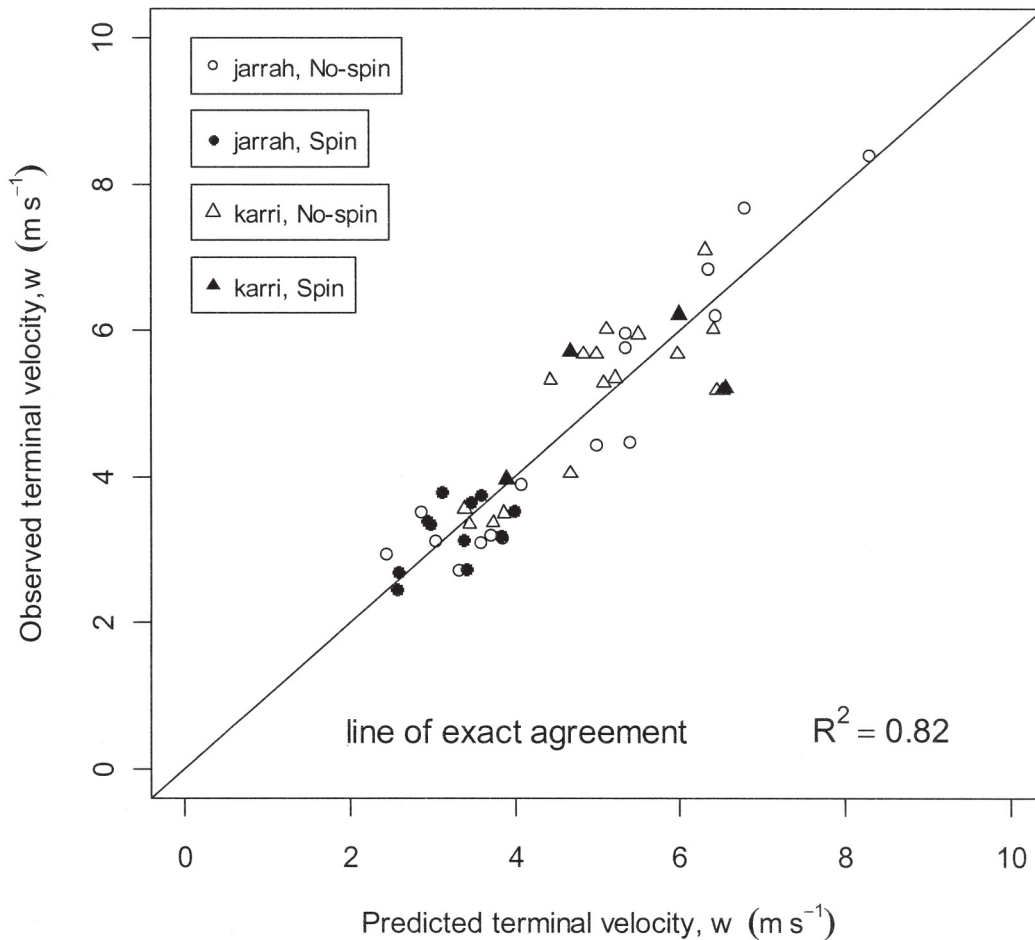


Figure 2. Observed terminal velocity vs terminal velocity predicted using Equations 4 and 5 for jarrah and karri bark samples, respectively.

Determinants of spin

Of the measured variables in Table 2, anova showed that *Species* ($p=0.04$), w ($P<0.02$) and Cd ($P<0.0001$) were the significant variables for *Spin*. It is argued here that *Spin* effectively increases drag and hence reduces terminal velocity. None of the variables for sample dimensions and mass were found to predict *Spin* although the karri samples which exhibited *Spin* had significantly smaller areas (Table 3, $df = 17$, $p = 0.003$), and significantly greater values for α (Table 3, $df = 4$, $p = 0.03$), than those which did not. *Spin* occurred rarely in karri samples, and only if α exceeded $1.24 \text{ kg}^{0.5} \text{ m}^{-1}$. *Spin* was more common in jarrah samples, but only if α was less than $1.02 \text{ kg}^{0.5} \text{ m}^{-1}$ (Table 3).

The effect of spin on terminal velocity

Equations 4 and 5 show that *Spin* reduces the terminal velocity of samples significantly. For example, for a jarrah sample, *Spin* would reduce terminal velocity by approximately $0.74 \pm 0.44 \text{ m s}^{-1}$ (Equation 4), compared to a No-spin sample. Evidence of aerodynamic lift in this study would be indicated by significantly higher values for C_d (Guries and Nordheim 1984), as shown in Table 3. The magnitude of the effect of increased drag can be confirmed using Equation 2. The mean value for C_d of the populations No-spin and *Spin* were 0.82 and 1.20 ($df =$

20, $P = 0.0006$), respectively, using a standard “*t*” test. Increasing the coefficient of drag from 0.80 to 1.20 represents a change of about 50%, and this would result in a decrease in terminal velocity of about 18% (Equation 2).

Discussion

All samples appeared to adopt a fall position of maximum drag as previously reported (Tarifa *et al.* 1965; 1967). Although many of the flat or cylindrical samples in this study exhibited gliding descent this was invariably in a spiral pattern. From these observations it appears unlikely that such pieces of bark would continue to glide in one direction. Thus gliding would not contribute significantly to the horizontal distance gained during descent. It appears probable that bark which falls in a wide spiral could add a maximum distance of less than 10 m the horizontal distance gained by an equivalent but non-gliding sample.

However, it is possible that for a certain bark shape and wind conditions, gliding could contribute significantly.

The shape of these samples may also influence the behaviour of similar pieces within a convection column.

Lee and Hellman (1969) found that the lower drag of flat plates tended to stabilize them within a swirling convection column rather than eject them. This finding suggests that the above samples of eucalypt bark, many of which are flat to curved plates, could behave similarly.

The range of terminal velocities was similar to that established by others. Tarifa *et al.* (1967) found that the initial terminal velocities for flat wood plates ranged from 2 m s⁻¹ for balsa samples to more than 14 m s⁻¹ for oak samples. Clements (1977) derived a value of 5.6 m s⁻¹ for undescribed samples of birch paper bark (*Betula papyrifera* Marsh.) and noted that they would remain in a flaming state at their terminal velocity. More than 20 of the 49 eucalypt bark samples tested in this study had terminal velocities of between 2.5 and 4.0 m s⁻¹. Because these terminal velocities are less than the convection updraft of bushfires of low to moderate intensity, the samples could be detached from trunks, say, and lofted above such fires. If such samples remained alight they could cause spotting beyond the burn perimeter. Most samples had terminal velocities of less than 6.9 m s⁻¹, and thus could be lofted in the convection plume of fires of moderate to high intensity.

The root of surface density (α) was shown to be the most significant explanatory variable for terminal velocity, as could be expected for a falling particle (Equation 2). Terminal velocities for jarrah samples were well-predicted using variables α and Spin (Equation 4, Figure 2), and less well-predicted for karri (Equation 5, Figure 2). This difference is probably due to the greater variability in shape of the karri samples.

The mean derived values for coefficient of drag for No-spin samples of karri and jarrah were 0.85 and 0.77, respectively (Table 3). These values are significantly less than the value of 1.17 modelled for wooden disks (Anthenien *et al.* 2006), and the standard value of approximately 1.0 for flat plates. This difference has several implications. It is likely that the derived values of C_d are valid and that they are relatively low because of the streamlining effect of the curvature of the bark samples. Alternatively, the derived values could be invalid and relatively low because the measured values for A (Table 1) overestimate the effective area presented to the airflow.

The property of *Spin* provided aerodynamic lift which significantly increased the coefficient of drag and could effectively reduce terminal velocity by almost 20%. This finding parallels work by Norberg (1973) and Guries and Nordheim (1984) on the effect of autorotation on the terminal velocities of maple samaras. Spin was common in jarrah samples, but only for samples with low surface densities.

Although this study shows some differences in free-fall behaviour between species, these are insufficient to explain differences in observed spotting behaviour. Available data on annual bark shed and bark consumption by fire are also insufficient to explain differences in spotting behaviour. Anecdotal evidence suggests that long-unburnt jarrah trunks and branches accumulate significantly more, thin, loosely attached bark flakes than do karri trunks. Such a difference, together with the fact that one third of the jarrah flakes had terminal velocities less than the minimum of the karri

flakes, could partly explain the observed differences in spotting behaviour. The rate of combustion of a firebrand affects the rate at which terminal velocity is reduced and the heat flux available to ignite a fuelbed on landing. Fast-burning firebrands will lose terminal velocity quickly and be easily transported, and, although their potential spotting distance will be reduced due to their consumption rate, will have a greater likelihood of igniting a fuelbed than slow-burning firebrands. Ellis (2000) found that for samples burning at their terminal velocities, bark of messmate stringybark (*E. obliqua* L'Her.) could have flaming times of 20 s or more, and quickly lost terminal velocity. In comparison, samples of a gum-barked type (bluegum, *E. globulus* subsp. *bicostata* Maiden, Blakely & J. Simm.) tended to have flaming times of zero or a few seconds and combust very slowly (Ellis 2000). Slowly combusting firebrands can potentially cause spotting at longer distances than fast-burning firebrands. It is likely that the combustion patterns for jarrah and karri have some similarities with the observations made for messmate and bluegum bark. It is also likely that the fibrous jarrah flakes on trunks and branches, which may be weathered for years, would ignite more easily than karri bark, which tends to be shed annually, and hence would be less weathered.

Conclusions

Most samples had terminal velocities sufficiently low for them to be lofted in the convection column of low to moderate intensity fires. The low terminal velocities of jarrah and karri bark flakes are due to low surface densities, sometimes coupled with the effect of fast spin. The lowest terminal velocities were achieved by jarrah samples, and this was due to these two properties. The karri samples showed relatively poor correlation with root of surface density, apparently because of the variability in sample shape, and hence coefficient of drag. Observed differences in spotting behaviour between the two species are their spotting densities and maximum spotting distances (Cheney and Bary 1969). Measured differences in free-fall behaviour are insufficient to explain observed differences in spotting behaviour. Additional differences between species which are likely to explain spotting observed spotting behaviour are the numbers of detachable flakes, their ease of ignition, and their combustion characteristics and pattern of loss of terminal velocity during flight.

Acknowledgements: I would like to thank Phil Cheney and Stuart Matthews of CSIRO Sustainable Ecosystems, and Ben Miller of the Botanic Gardens and Parks Authority of Western Australia, for their thorough reviews. John Owen of CSIRO facilitated the use of the mobile tower.

References

- Albini F A 1979 Spot fire distance from burning trees – a predictive model. General Technical Report INT-56, USDA Forest Service, Ogden, Utah.
- Anthenien R A, Tse S D & Fernandez-Pello A C 2006 On the trajectories of embers initially elevated or lofted by small-scale ground fire plumes in strong winds. *Fire Safety Journal* 41 Issue 5: 349–363.

- Cheney N P & Bary G A V 1969 The Propagation of Mass Conflagrations in a Standing Eucalypt Forest by the Spotting Process. Paper A6, Mass Fire Symposium, Canberra, February 1969, Commonwealth of Australia.
- Clements H B 1977 Lift-Off of Forest Firebrands. USDA Forest Service Research Paper SE-159.
- Ellis P F 2000 The aerodynamic and combustion characteristics of eucalypt bark – a firebrand study. PhD thesis, Australian National University.
- Gould J S, McCaw W L, Cheney N P, Ellis P F, Knight I K & Sullivan AL 2008 Project Vesta: Fire in Dry Eucalypt Forest: Fuel Structure, Fuel Dynamics and Fire Behaviour. CSIRO / Dept. of Environment & Conservation, Western Australia.
- Guries R P & Nordheim E V 1984 Flight Characteristics and Dispersal Potential of Maple Samaras. *Forest Science* Vol. 30, No. 2: 434–440.
- Lee S L & Hellman J M 1969 Study of firebrand trajectories in a turbulent swirling natural convection plume. *Combustion and Flame* 13: 645–655.
- Luke R H & McArthur A G 1978 Bushfires in Australia. CSIRO Division of Forest Research, Australian Government Publishing Service, Canberra.
- Marks L S (ed) 1951 *Mechanical Engineers' Handbook*. McGraw-Hill, New York.
- McArthur A G 1967 Fire behaviour in eucalypt forests. Commonwealth of Australia Forestry and Timber Bureau Leaflet No. 107.
- McCarthy G J & Tolhurst KG 1998 Effectiveness of Firefighting First Attack Operations, Department of Conservation & Natural Resources, 1991/92-1994/95 Research Report No. 45. Department of Natural Resources & Environment, Victoria.
- McCaw W L, Simpson G & Mair G 1992 Extreme fire behaviour in 3-year-old fuels in a Western Australian mixed Eucalyptus forest. *Australian Forestry* 55, 107–117.
- Muraszew A 1974 Firebrand Phenomena. Aerospace Report ATR-74(8165-01)-1. The Aerospace Corporation, El Segundo, California.
- Muraszew A, Fedele J B & Kuby W C 1975 Firebrand investigation. Aerospace Report ATR-75(7470)-1. The Aerospace Corporation, El Segundo, California.
- Muraszew A, Fedele JB & Kuby WC 1976 Investigation of fire whirls and firebrands. Aerospace Rep. ATR-76(7509)-1, The Aerospace Corporation, El Segundo, California.
- Muraszew A & Fedele JB 1976 Statistical Model for Spot Fire Hazard. Aerospace Rep. ATR-77(7588)-1, The Aerospace Corporation, El Segundo, California.
- Norberg R A 1973 Autorotation, self stability, and structure of single-winged fruits and seeds (samaras) with comparative remarks on animal flight. *Biological Reviews*, 48:561–596.
- O'Connell A M & Menagé P M A 1982 *Australian Ecology*, Volume 7, Issue 1, 49–62. The Ecological Society of Australia Inc.
- Raupach M R 1990 Similarity analysis of the interaction of bushfire plumes with ambient winds. *Mathematical Computer Modelling*, Vol. 13, No.12: 113–121.
- Tarifa C S, del Notario P P & Moreno F G 1965 On the Flight Paths and Lifetimes of Burning Particles of Wood. Tenth Symposium (International) on Combustion: 1021–1037.
- Tarifa C S, del Notario P P, Moreno F G & Villa A R 1967 Transport and Combustion of Firebrands. Final Report of Grants FG-SP-114 and FG-SP 146, Aeronautical Institute of Madrid for USDA.
- Tolhurst K G & MacAulay A S 2003 SAROS – a model for predicting the effect of mass spotting on the rate and spread of forest fire. 3rd Int. Wildland Fire Conference and 10th Annual AFAC Conference, 2–6 October 2003, Sydney, Australia.